Effect of subsurface damages in the seed crystal on the crystal quality of 4H-SiC single crystals grown by the PVT technology

Guofeng Li [a, b], Wei Hang [a], Hongyu Chen [a], Rong Wang [b, c, *], Xiaodong Pi [b, c, *], Deren Yang [b, c], Julong Yuan [a, *]

[a] Ultra-precision Machining Research Center & College of Mechanical Engineering, Zhejiang University of Technology, Hangzhou 310023, China

[b] Institute of Advanced Semiconductors & Zhejiang Provincial Key Laboratory of Power Semiconductor Materials and Devices, Hangzhou Innovation Center, Zhejiang University, Hangzhou, Zhejiang 311200, China

[c] State Key Laboratory of Silicon and Advanced Semiconductor Materials & School of Materials Science and Engineering, Zhejiang University, Hangzhou, Zhejiang 310027, China

ABSTRACT

This paper focuses on the generation and transformation of defects associated with subsurface damages (SSDs) in seed crystals during the physical vapor transport (PVT) growth of 4H-SiC crystals. SSDs in the 4H-SiC seed crystal are firstly revealed and labeled by photo-chemical etching. After 30 min of the PVT growth on the 4H-SiC seed crystal, we find that the ridge-like scratches with the height ranging from 0.2 to1.5 μm are formed in the region above the SSDs in the 4H-SiC seed crystal. Raman spectra analysis that these ridge-like scratches are 4H-SiC with tensile strain. We then continue the PVT growth to obtain a 4H-SiC boule, and carry out the wafering process to obtain 4H-SiC single-crystal wafers. For the bottom wafer above the 4H-SiC seed wafer, the full width at half maximum (FWHM) of the rocking curves of the region above the SSDs of the seed wafer is higher than other regions, indicating the SSDs degrade the crystalline quality of 4H-SiC single crystal. The average value of the FWHM of the rocking curves of the top wafer becomes lower than that of the bottom wafer, indicating that the effect of SSDs gradually recovers. Molten-KOH etching indicates that SSDs in the 4H-SiC seed crystal give rise to the formation of low-angular grain boundaries (LAGBs), that consists of wall of threading edge dislocations

* Corresponding authors.
E-mail addresses: rong_wang@zju.edu.cn (R. Wang), xdpi@zju.edu.cn (X. Pi), jlyuan@zjut.edu.cn (J. Yuan)

(TEDs), in 4H-SiC single crystals.

Keywords: 4H silicon carbide, subsurface damages, physical vapor transport growth, crystalline defects

1. Introduction

4H silicon carbide (4H-SiC) has attracted great attention in high-power, high-frequency and high-temperature electronics, due to the exceptional properties such as wide bandgap, high breakdown electric field strength, high electron mobility and high thermal conductivity [1, 2]. The physical vapor transport (PVT) technology, which has the advantages of equipment simplicity, low cost of consumables, and technology maturity, has become the mainstream technology to grow 4H-SiC crystals [3]. The PVT growth of 4H-SiC single crystals are motivated by the temperature gradient between the 4H-SiC seed crystal and the SiC powder. During the nucleation of 4H-SiC single crystals on the seeds, defects are usually incorporate into 4H-SiC single crystals as a result of subsurface damages (SSDs) in 4H-SiC single-crystal seeds.

The processing of 4H-SiC wafers includes wire sawing, grinding, lapping and polishing. The grinding, lapping and polishing are expected to sequentially remove the damage layer introduced by the wire sawing, to achieve the global and local planarization of 4H-SiC wafers free of damages and low surface roughness[4]. Nevertheless, the processing of 4H-SiC wafers suffers from the problem of incomplete removal of processing damages or unavoidable introduction of new damages, which in turn seriously affect the subsequent growth and the quality of epitaxial layers [5]. It has been proposed that SSDs can be exposed by combining photo-chemical etching and molten-alkali etching [6, 7]. However, the effect of SSDs in the seed crystal on the crystal quality of 4H-SiC single crystals is still ambiguous.

In this work, we investigate the effect of SSDs in 4H-SiC seed crystals on the crystal quality of 4H-SiC single crystals grown by the PVT technology. It has been found that ridge-like scratches with the height ranging from 0.2 to1.5 μm are formed in the region above the SSDs in the 4H-SiC seed crystal after 30 min of PVT growth. These ridge-like scratches are 4H-SiC with tensile strain. After the whole PVT and wafering process, we obtain 4H-SiC single-crystal wafers. For the bottom wafer above the 4H-SiC seed wafer, the full width at half maximum (FWHM) of the rocking curves of the region above the SSDs of the seed wafer is higher than other regions, indicating the SSDs degrade the crystalline quality of 4H-SiC single crystal. The average value of the FWHM of the rocking curves of the top wafer becomes lower than that of the bottom wafer, indicating that the effect of SSDs gradually recovers. Molten-KOH etching indicates that SSDs in the 4H-SiC seed crystal give rise to the formation of low-angular grain boundaries (LAGBs), that consists of wall of threading edge dislocations (TEDs), in 4H-SiC single crystals.

2. Experimental Procedure

2.1 Methods

A 4-inch 4H-SiC single crystal was used as the seed crystal of the PVT growth. Before crystal growth, photochemical etching was used to reveal SSDs of the 4H-SiC seed crystal. Using a mercury lamp as the UV light source, the seed crystal was etched in a 0.05 M KOH solution for 20 min to check the presence of SSDs. The seed crystal was then subjected to chemical-mechanical polishing (CMP) until the damage was not visible under the optical microscope.

After CMP, the seed crystal was used to grow 4H-SiC single-crystal boule grown by the PVT technology, with the temperatures in the range of 2200 to 2300 °C and pressures in the range of 1 to 10 mbar. N-type doping was achieved by mixing high-purity N_2 in argon (Ar) as the doping source. The PVT growth were divided into two stages to observe the effect of SSDs on the crystal quality of 4H-SiC single crystals. For the first stage, we investigated the effect of SSDs on the crystal quality at the seed and growth interface. For the second stage, we focused on the changes of the crystal defects induced by SSDs during the single crystal growth by continuing the growth thickness up to 10 mm. After the PVT growth, 4H-SiC wafers were obtained by slicing, lapping and CMP successively. The top and bottom wafers were etched by molten KOH etching at 550°C for 10 min to reveal dislocations on the surface of 4H-SiC.

2.2 Characterizations

Before the experiment, the wafer inspection system (Lasertec, SICA82) was used to statistically distribute the defects of 4H-SiC seed crystal after CMP treatment. The surface morphology of the crystals after 30 min of growth and the surface morphology of the etched the top and bottom wafers were examined by optical microscope (OM) (Olympus, BX53M) and white light interferometer (WLI) (Bruker, ContourX-200). The Raman spectra were measured by the Raman spectrometer (Horiba, LabRAM

Odyssey). The high-resolution X-ray diffraction (HRXRD) rocking curve measurements were performed on the XRD diffractometer (Malvernpanalytical, X' PERT 3 MRD) operated with Cu Kα1 radiation. Dislocations after molten KOH etching were counted by the optical microscope (FabXLab).

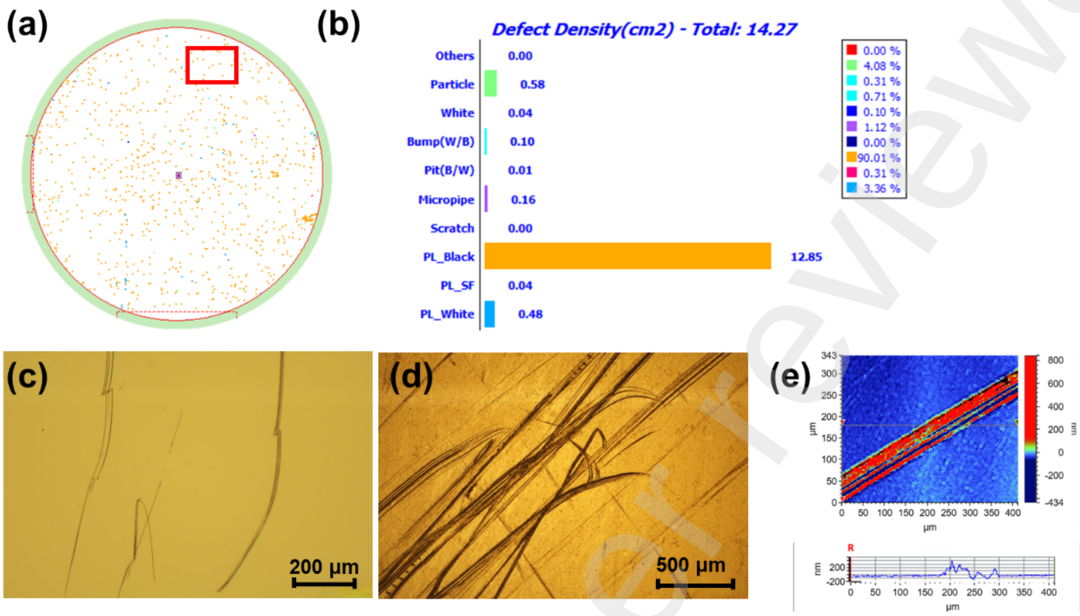

Fig. 1 (a) The distribution and (b) density of defects in 4H-SiC seed crystals. (c) The OM morphology of SSDs on the surface after photochemical etching of the seed. (d) The OM morphology of the crystal surface after 30 min of growth by the PVT and (e) its localized WLI image.

3. Result and Discussion

3.1 Generation of defects associated with SSDs at the early stage of PVT growth

Fig. 1(a) and Fig. 1(b) demonstrate the distribution and density of defects on the Si face of CMP-treated 4H-SiC seed crystal. Although most of the defects such as scratches, pits, bumps, and particles are successfully controlled after CMP, the UV-PL image reveals high density of PL-Black defects on the Si surface of CMP-treated 4H-SiC seed crystal. However, we observe linear PL-black defects on the Si face of the CMP-treated 4H-SiC seed crystal. These linear PL-Black defects are not visible under OM, but they appear as straight lines under UV-PL measurements. The term 'PL-black' refers to non-radiative recombination of photo-generated carriers. Similar to what happens in Ref. [6], we reveal these SSDs in 4H-SiC seed crystal by employing photochemical etching to clarify the nature of the SSDs. Fig. 1(c) displays the OM image of the SSDs after photochemical etching, which corresponds to the region of relatively high-density PL-Black region in Fig. 1(a). In order to understand the effect of SSDs on the seed crystal on the crystal quality of 4H-SiC single crystals, we carry out CMP of the seed crystal to remove SSDs, and use the same seed crystal to grow 4H-SiCsingle crystal by the PVT technology.

To investigate the effect of SSDs in the seed crystal on the initial crystal quality of 4H-SiC single crystals, we stop the PVT growth, and investigate the surface morphologies of the 4H-SiC single crystal. Fig. 1(d) shows that after 30 minutes of the PVT growth, there exists scratch-like substances on the same region of the SSDs in the 4H-SiC seed crystal. The three-dimensional (3D) morphologies of these scratch-like lines is presented in Fig. 1(e). It is clear that the 3D morphologies of the so-called scratch-like substances are actually ridge-like structures with the height ranging from 0.2 to1.5 μm, while the other regions have smooth surfaces with a Roughness Average (Ra) of 80 nm. Considering the shape and the location of the scratch-like substances in the grown crystal overlap with the SSDs in the seed crystal, the scratch-like lines might be caused by SSDs in the seed crystal.

Raman measurements are then used to characterize the crystal quality of 4H-SiC across the scratch-like lines. The standard Raman spectra of 4H-SiC is shown in Fig. 2(a). The peaks locating at 204 cm^{-1}, 776 cm^{-1}, and 980 cm^{-1} correspond to the first order of the folded modes of the transverse acoustic branch (FTA), transverse optical branch (FTO), and the longitudinal optical branch (FLO) of 4H-SiC, respectively. These peaks can be used to characterize the crystalline quality, internal stresses, phase transitions, and other related properties of 4H-SiC [8]. Fig. 2(c) presents the Raman spectra of the defect and non-defect regions of 4H-SiC in the initial growth stage. It is clear that both the defective and non-defective regions exhibit characteristic Raman peaks, confirming the presence of 4H-SiC polymorph. The Raman spectra in Fig. 2(d) and Fig. 2(e) exhibit the Raman characteristic peaks at 204 cm^{-1} and 776 cm^{-1}. These peaks indicate that the values of the full width at half maximum (FWHM) of the 204 cm^{-1} is larger in the defect region compared to the non-defect region. The broadening of the FTA peak indicates the degradation of the crystal quality in the defective region. The positive and negative shifts of the peak of the FTO mode indicate the compressive and tensile residual stresses, respectively [9]. In contrast to the non-defective regions, the FTO peak shifts to lower wavelengths in the defective regions with large offset values, which indicates the presence of large tensile stresses in the defective regions. During the PVT growth, the ambient gas phases such as Si, Si_2C, and SiC_2 exhibit a preference to aggregate and react, leading to nucleation at the defective area. One of the main reasons for this change in the growth mode is the presence of higher levels of stress in the defective region [10]. At the initial PVT growth stage of the 4H-SiC single crystal, the spiral growth mode of the step spreading from the facet region has not yet fully developed. Due to the imperfect spiral growth mode, there exists higher density of dislocations caused by the SSDs in 4H-SiC seed crystals. This, in turn, results in higher energy accumulation in these regions.

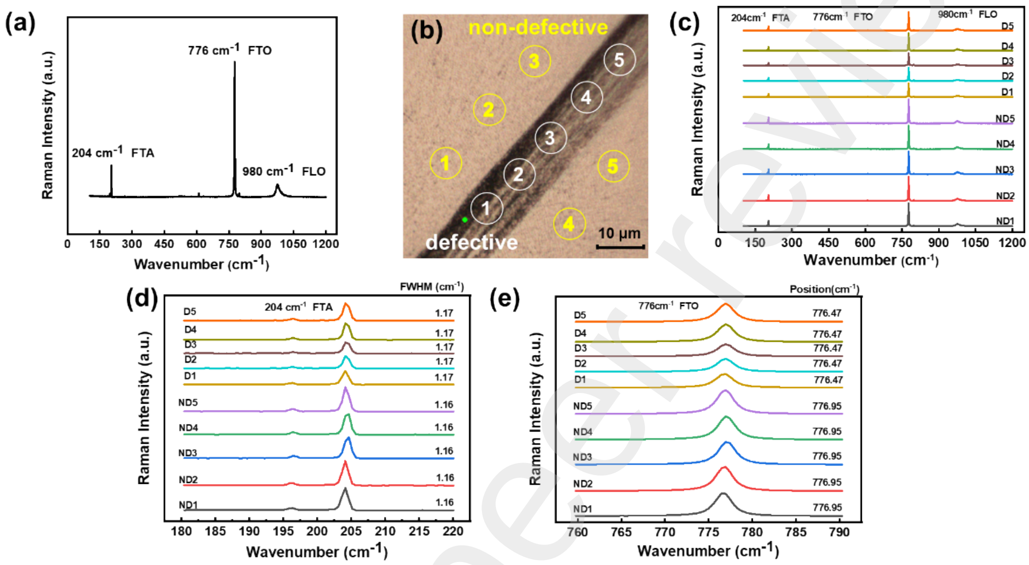

Fig. 2 (a) The Raman spectra of 4H-SiC. The Raman spectra of 4H-SiC grown around the SSDs of the seed crystal after 30 min of growth. (d) The Raman spectra around 204 cm^{-1} and (e) 776 cm^{-1} characteristic peak corresponding to the positions indicated in (b).

3.2 Evolution of defects caused by SSDs as the PVT growth proceeds

By comparing the top and bottom wafers of the crystal, we can explore the evolution of defects corresponding to SSDs in the seed crystal as the growth proceeds. Fig. 3 presents the HRXRD rocking curves of the top and bottom 4H-SiC wafers, with the points taken shown in Fig. 3(c). As shown in Fig. 3(a) and Fig.3(b), the shape of the rocking curve of the top 4H-SiC wafer more closely resembles the Gaussian form when compared with the bottom 4H-SiC wafer. The rocking curves of the bottom wafer have different shapes and even appear bimodal, suggesting that the polymorph of SiC may have changed in this region [11]. Since the rocking curve of XRD can reflect the crystallinity of the crystal [12], the crystallization of 4H-SiC is enhanced as the PVT growth proceeds. This indicates that the effect of SSDs in the seed crystal gradually decreases as the PVT growth proceeds. Meanwhile, the FWHM statistics of each point of the top and bottom wafers in Fig. 3(d) show that the FWHM of the rocking curves of the bottom wafer is generally larger than that of the top wafer. However, there are also singularities where the FWHM of the bottom wafer is larger than that of the top wafer, which may be caused by other defect factors in the crystal.

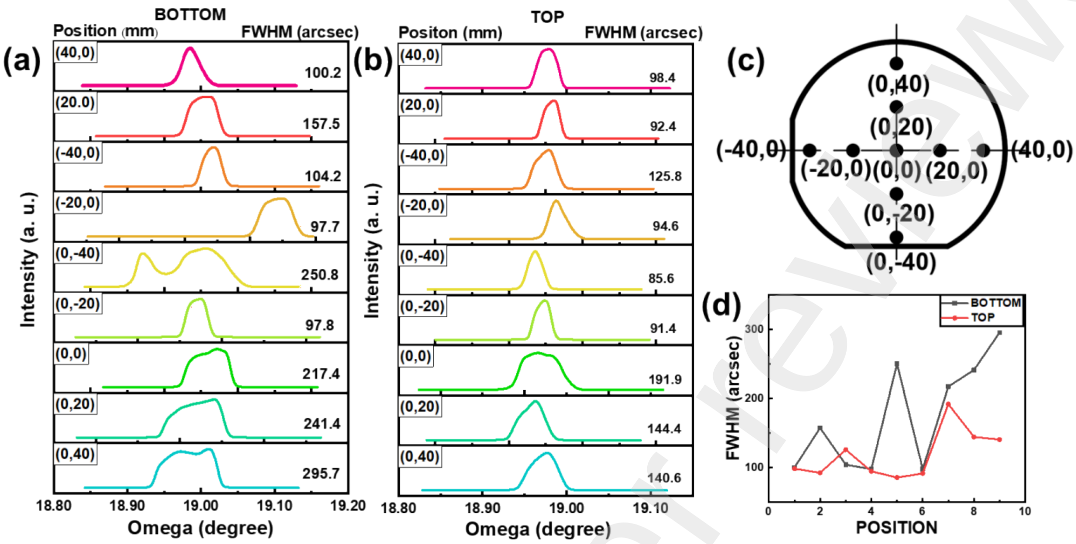

Fig.3 Rocking curves of HRXRD corresponding to the (a) bottom and (b) top wafers of 4H-SiC at the (c) pickup points position, and their FWHM statistics are shown in (d).

Molten KOH etching is then employed to reveal dislocations in 4H-SiC wafers to investigate the effect of SSDs in the seed crystal on the distribution of dislocations in PVT-grown 4H-SiC single crystals. The top and bottom wafers were etched separately in molten KOH for 10 min. Fig. 4(a) displays the surface morphology of the growth after 30 minutes, while Fig. 4(b) and Fig. 4(c) show the morphologies of the molten KOH etched top and bottom wafers. The distribution of defects within the crystal after 30 minutes of growth can be roughly characterized by the results of the bottom wafer. Compared with the bottom wafer, both the distribution and density of the etching pits were optimized after the molten KOH etching of the top wafer, indicating that defects such as dislocations have gradually disappeared during growth, leading to an improvement in the crystal quality. Additionally, a similar morphological pattern was observed in the upper right corner of the figure, whether after 30 minutes of growth or molten KOH etching of the top and bottom wafers. The pattern's shape is "N"-shaped, resembling the pattern of grain boundaries shown in Fig. 4(d), Fig. 4(e), and Fig. 4(f). Fig. 4(g) and Fig. 4(h) show the zoom-in image of this defective region, marked by the red line in reveals that the defects at the marking location are formed by a large number of aggregated TED dislocations. Previous studies have reported LAGBs resulting from the aggregation of a large number of TEDs, leading to the appearance of a dislocation walls phenomenon [13]. Combining with the previous speculations, it can be determined that the defects associated with the "N"-shaped pattern are LAGBs generated during growth.

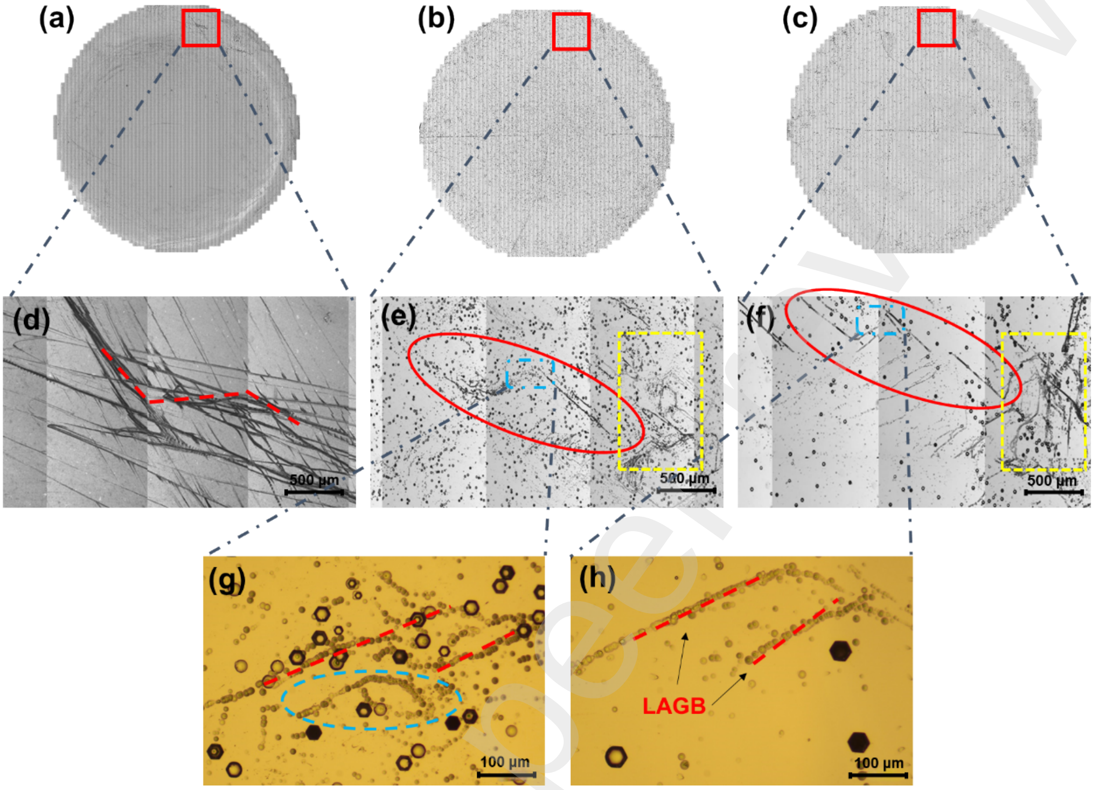

Fig. 4 (a) Morphology of the crystal surface after 30 min of PVT growth. Surface morphologies of etched (b) bottom and (c) top wafers after 5 h of PVT growth. (d)-(f) Zooming in surface morphologies of the same positions in Figs. (a)-(c), respectively. Fig. (g) and (h) show localized magnified views of similar LAGBs in bottom and top wafers, respectively.

During the early stage of crystal growth, the mode of growth was predominantly dominated by the preferential growth of crystals at SSDs, supplemented by growth along the direction of the step. This leads to a deviation of the crystals grown in the two modes. Especially near the interface of the two crystals, stresses coalesce. Due to this internal stress, in the early stages of growth, different growth centers are dislocated and tilted against each other, leading in turn to elastic deformation of crystals grown at two different rates to accommodate lattice tilting or the formation of LAGBs.

As mentioned before, dislocations on 4H-SiC wafers would gradually decrease along the crystal growth direction [14, 15]. However, in Fig. 4(b) and Fig. 4(c), there are still a large number of etching pits visible near LAGBs. This is because LAGBs can induce dislocation nucleation. LAGBs provide additional surface energy that can serve as nucleation sites for crystal growth. The more nucleation sites grow, the easier dislocations, including TEDs, BPDs, and TSDs, can form. However, this does not mean that the region would remain a high defect density in growth, as LAGBs were not constant over time, and they would change according to the environmental factors affecting crystal growth. It can be noticed that the LAGBs, which could be observed in the bottom wafer, have completely disappeared in the top wafer, as shown by the blue wireframe markings in Fig. 4(g). This phenomenon can be explained by the mechanism of dislocation conversion. The main components of LAGBs in this study are TEDs. When TEDs encounter approaching macro-steps (formed on off-axis grown crystals by step bunching), the TEDs are deflected due to the overgrowth of the macro-steps and can only be deflected to the basal plane in the direction of the step flow because the macro-steps do not allow dislocations to enter their structure[16]. As the crystal grows, the edge-type dislocations were gradually converted from TEDs to BPDs, resulting in the gradual disappearance of LAGBs.

4. Conclusion

In summary, we have investigated the effect of SSDs in the seed crystal on the crystal quality of PVT-grown 4H-SiC single crystals. The research indicates that the existence of SSDs results in the development of significant internal stresses and compromised crystal quality, along with noticeable macroscopic defects like LAGBs, within the specified region during the process of 4H-SiC crystal growth. At the initial stages of growth, SSDs in the seed crystal increase the local surface energy, leading to preferential nucleation of crystals with high-energy surfaces. Consequently, the dominant growth mode is characterized by growth along these high-energy surfaces. However, at this time, especially in the denser region of SSDs, the grown crystals of the two modes are misaligned and tilted in their growth centers due to different growth rates and other reasons, which in turn form obvious LAGBs. By molten KOH etching, we succeeded in revealing the etch pit morphology of LAGBs in crystals grown in proximity to SSDs. We found that LAGBs are dislocation walls formed by the aggregation of a large number of TEDs, and that SSDs increase the densities of dislocations such as TEDs in the crystals. As a result, there are extremely high dislocation densities of TEDs and BPDs in the vicinity of LAGBs. Our work indicates that careful wafering process should be designed to avoid the presence of SSDs in the seed crystals to improve the quality of PVT-grown 4H-SiC single crystals. It also provides a new basis for identifying the origin of LAGBs in 4H-SiC wafers.

CRediT authorship contribution statement

Guofeng Li: Conceptualization, Investigation, Writing – original draft. **Wei Hang**: Writing - Review & Editing. **Hongyu Chen**: Writing - Review & Editing. **Rong Wang**: Writing – original draft, Supervision. **Xiaodong Pi**: Funding acquisition, Writing - Review & Editing. **Deren Yang**: Funding acquisition. **Julong Yuan**: Supervision.

Declaration of Competing Interest

The authors declare that they have no known competing financial interests or personal relationships that could have appeared to influence the work reported in this paper.

Data availability

Data will be made available on request.

Acknowledgement

This work is supported by National Natural Science Foundation of China (Grant Nos. 62274143, U22A2075, 12204161, 52275467, 52375468), “Pioneer” and “Leading Goose” R&D Program of Zhejiang (Grant No. 2022C01021), National Key Research and Development Program of China (Grant No. 2018YFB2200101), Fundamental Research Funds for the Central Universities (Grant No. 2018XZZX003-02), Natural Science Foundation of China for Innovative Research Groups (Grant No. 61721005), and National Key Research and Development Program of China (2023YFE0202900).

Reference

[1] H. Matsunami. Technological breakthroughs in growth control of silicon carbide for high power electronic devices. Japanese Journal of Applied Physics. 43(10) (2004) 6835-6847. https://doi.org/10.1143/jjap.43.6835

[2] T. Kimoto and H. Watanabe. Defect engineering in sic technology for high-voltage power devices. Applied Physics Express. 13(12) (2020). https://doi.org/10.35848/1882-0786/abc787

[3] Y. M. TAIROV and V. F. TSVETKOV. Investigation of growth processes of ingots of silicon carbide single crystals. Journal of Crystal Growth. 43 (1978) 209-212. https://doi.org/10.1016/0022-0248(78)90169-0

[4] J. ZHANG, *et al.* Wire saw slicing and its application in silicon carbide wafers processing. Journal of Synthetic Crystals. 52(03) (2023) 365-379. https://doi.org/10.16553/j.cnki.issn1000-985x.2023.03.001

[5] H. Sako, *et al.* Characterization of scraper-shaped defects on 4h-sic epitaxial film surfaces. Japanese Journal of Applied Physics. 53(5) (2014). https://doi.org/10.7567/jjap.53.051301

[6] W. Geng, *et al.* Identification of subsurface damage of 4h-sic wafers by combining photo-chemical etching and molten-alkali etching. Journal of Semiconductors. 43(10) (2022). https://doi.org/10.1088/1674-4926/43/10/102801

[7] Q. Shao, *et al.* Nucleation of threading dislocations in 4h-sic at early physical-vapor-transport growth stage. Crystal Growth & Design. 23(7) (2023) 5204-5210. https://doi.org/10.1021/acs.cgd.3c00416

[8] X. Liu, *et al.* Crack healing behavior of 4h-sic: Effect of dopants. Journal of Applied Physics. 133(14) (2023). https://doi.org/10.1063/5.0140922

[9] J. Zhang, *et al.* Effect of hexagonality on the pressure-dependent lattice dynamics of 4h-sic. New Journal of Physics. 24(11) (2022). https://doi.org/10.1088/1367-2630/ac9c79

[10] J. Drowart, *et al.* Thermodynamic study of sic utilizing a mass spectrometer. The Journal of Chemical Physics. 29(5) (1958) 1015-1021. https://doi.org/10.1063/1.1744646

[11] N. Zhang, *et al.* Physical-vapor-transport growth of 4h silicon carbide single crystals by a tiling method. Journal of Crystal Growth. 600 (2022). https://doi.org/10.1016/j.jcrysgro.2022.126915

[12] A. Ruammaitree, *et al.* Determination of non-uniform graphene thickness on sic (0001) by x-ray diffraction. Applied Surface Science. 282 (2013) 297-301. https://doi.org/10.1016/j.apsusc.2013.05.122

[13] N. Ohtani, *et al.* Behavior of basal plane dislocations in hexagonal silicon carbide single crystals grown by physical vapor transport. Japanese Journal of Applied Physics. 45(3A) (2006) 1738-1742. https://doi.org/10.1143/jjap.45.1738

[14] X. F. Chen, *et al.* Reduction of dislocation density of sic crystals grown on seeds after h2 etching. Materials Science Forum. 897 (2017) 19-23. https://doi.org/10.4028/www.scientific.net/MSF.897.19

[15] I. G. Yeo, *et al.* Study on dislocation behaviors during pvt growth of 4h-sic. Materials Science Forum. 963 (2019) 64-67. https://doi.org/10.4028/www.scientific.net/MSF.963.64

[16] M. Dudley, *et al.* Stacking faults created by the combined deflection of threading dislocations of burgers vector c and c+a during the physical vapor transport growth of 4h–sic. Applied Physics Letters. 98(23) (2011). https://doi.org/10.1063/1.3597226